JOURNAL OF MATERIALS SCIENCE: MATERIALS IN MEDICINE **16** (2005) 37–45

Microneedles coated with porous calcium phosphate ceramics: Effective vehicles for transdermal delivery of solid trehalose

M. SHIRKHANZADEH
Department of Mechanical and Materials Engineering, Queen's University, Nicol Hall, 60 Union Street, Kingston, Ontario, K7L 3N6, Canada

Trehalose (α-D-glucopyranosyl-α-D-glucopyranoside) is recognized as a promising fast-dissolving solid reservoir capable of stabilizing the native structure of proteins and suitable for loading with a wide variety of bioactive substances. Currently, there is a growing interest in developing cost-effective methods for immobilizing solid trehalose on arrays of microneedles for delivering protein-based and DNA-based vaccine to the epidermis. In the present work, micro-porous calcium phosphate coatings were used to provide a biocompatible interface with a large surface area for the effective immobilization of trehalose on microneedles. Calcium phosphate coatings with varying degrees of porosity were electrochemically synthesized on the tips of stainless steel acupuncture needles and loaded with solid trehalose. Skin experiments were designed to determine the ability of micro-porous calcium phosphate coatings to deliver solid trehalose into epidermis without breaking during insertion. The mechanical performance of the coatings was assessed by inserting the tips of the coated needles into human skin to an average depth of 100–300 μm and then removing them for analysis by scanning electron microscopy. Microporous calcium phosphate coatings loaded with trehalose effectively breached the stratum corneum and allowed direct access to the epidermis without breaking and without stimulating nerves in deeper tissues.

1. Introduction

In recent years increasingly sophisticated and potent protein-based and DNA- based vaccines have been developed by the biotechnology industry. Skin is considered to be an attractive target for delivery of these new vaccines. Skin is recognized as a highly immune-reactive tissue with a dense network of antigen-presenting cells (APCs), especially within the epidermis [1]. Targeting the epidermis, however, can be technically challenging due to the poor permeability of the outer 10–20 μm of the skin known as the stratum corneum (SC). The recent development of microneedles and microblades for transdermal drug delivery has emerged as an approach to enhance the poor permeability of the skin by creating microscale conduits for transport across the stratum corneum [2]. Using microfabrication technology, arrays of solid silicon microneedles have been fabricated with individual needles measuring 150 μm in length, 80 μm at the base, and a tip radius of curvature less than 1 μm that can penetrate the stratum corneum painlessly [2]. Devices consisting of arrays of metallic microneedles and microblades coated with solid biodegradable reservoirs containing therapeutic agents and vaccines have also been reported [3] which may find potential applications in rapid mass immunization programs. Preferred biodegradable solid reservoirs for use with these new devices are sugars, and in particular stabilizing sugars that form a glass such as lactose, raffinose, trehalose, or sacrose. Once the coated microneedles have pierced the stratum corneum and come to contact with body fluid, the agent can be released as a result of dissolution and biodegradation of the reservoir. Given the potential advantages of these new systems for vaccination, there is an increasing need for cost-effective methods such as inkjet printing to selectively dispense precise doses of vaccine formulations on specific regions of microneedles that penetrate skin. The application of such techniques, however, requires that the surface of tiny microneedles be modified to rapidly absorb and dry the liquid vaccine formulations in a short time.

Calcium phosphates and particularly stoichiometric and non-stoichiometric hydroxyapatite are known to be biocompatible materials. Previous work [4, 5] has demonstrated that microporous coatings consisting of interlocking calcium phosphate crystals with varying crystal sizes can be electrochemically fabricated on conductive substrates at relatively low temperatures. Due to their known biocompatibility and high capacity for water absorption, these porous coatings may provide

an attractive interface for immobilizing vaccine ingredients including antigens, adjuvants, and solid biodegradable reservoirs on microneedles. In order to be effective as vaccine carriers, however, these coatings need to have sufficient mechanical strength and should remain intact during penetration of microneedles through the stratum corneum.

In the present work, micro-porous calcium phosphate coatings with varying degrees of porosity were electrochemically fabricated on stainless steel acupuncture needles. Trehalose was incorporated into the porous calcium phosphate coatings as a model fast-dissolving antigen reservoir. The mechanical performance of the coatings with and without trehalose was assessed by inserting the tips of the coated needles into human skin and then removing them for analysis by scanning electron microscopy (SEM). Skin experiments were designed to determine the ability of microporous calcium phosphate coatings to effectively deliver solid trehalose into the epidermis without breaking during insertion. Trehalose was used as a model fast- dissolving reservoir because it is recognized as being a promising delivery vehicle capable of stabilizing the native structure of proteins and suitable for loading with a wide variety of bioactive substances [6].

2. Materials and methods

Sterilized stainless steel acupuncture needles (4 cm long, 200 μm diameter) with sharp tips having a radius of curvature of about 2 μm were used in this study. Microporous calcium phosphate coatings were deposited on these needles by the electrodeposition method described previously [4, 5]. Calcium phosphate coatings used in this study, their designations and preparation conditions, are summarized in Table I. Electrodeposition of calcium phosphates was carried out at 65 °C in a conventional electrolytic cell fitted with a platinum counter electrode and a saturated calomel electrode (SCE) acting as a reference electrode. Electrolytes with varying concentrations of calcium and phosphate ions from were prepared by dissolving reagent-grade Ca $(NO_3)_2$ and $NH_4H_2PO_4$ in deionized water. In all cases, the molar Ca/P ratio in the electrolytes was kept constant at 1.67. A Hokuto Denko (HD) HAB-151 potentiostat/galvanostat operating in potentiostatic mode was employed to maintain the potential of the needles (cathode) at pre-determined values with respect to SCE. The optimum potential for the uniform formation of the coatings was determined to be −0.9 volts with respect to the reference electrode. During the electrodeposition process, needles were dipped into the electrolyte to a depth of 0.5 cm, thereby limiting the coated region to the lower portion of the needles including the sharp tips.

TABLE I Microporous calcium phosphate coatings used in the study

Coating name	Electrolyte concentration ([Ca]), mM	Electrode potential (E), mV	Coating time (t), min
API	21	−0.9	5
APII	1	−0.9	120
APIII	0.5	−0.9	240

Needles coated with calcium phosphates for varying periods ranging from 5 min to 2 h were dried in a stream of air at room temperature and subsequently loaded with trehalose. Loading was achieved by dipping the coated needles in trehalose solutions to a depth of 0.5 cm for 1 min. Coated needles loaded with trehalose were then immediately dried in air at room temperature for 4 h and stored under dry conditions for 24 h before use.

The mechanical performance of the porous calcium phosphate coatings with and without trehalose was assessed by inserting the tips of the coated needles into the forearms of human volunteers who gave informed consent. The needle tips were inserted into skin to an average depth of approximately 100–300 μm for a short time (<30 s), and then removed for analysis by SEM. Due to the extreme sharpness of the needle tip, the coated needles penetrated the skin by applying only a gentle push. Generally, a needle will penetrate the skin when the pressure at the tip of needle has exceeded the skin's yield strength. The coated needles penetrated the skin by imposing a high level of strain to the stratum corneum that resulted in the local disruption of the SC and release of the intact corneocytes. SEM analysis of the needles removed from the skin revealed that the corneocytes released from the stratum corneum were often attached to the coated needles.

Thus, the presence of corneocytes attached to the coated needles allowed the minimum depth of penetration of needles to be determined by SEM. The mechanical stability of the coated needles was also tested under dry conditions by inserting the coated needles into a 300 μm thick latex film that was fixed to a plastic frame. SEM was employed to assess the extent of the surface morphological changes of the coated needles after piercing through the latex film.

Microporous calcium phosphate coatings with and without trehalose were also prepared on stainless steel plates (3×4 cm^2) for further characterizations. FT-IR spectroscopy was employed to study the chemical compositions of these coatings and to investigate the interactions between calcium phosphate crystals and trehalose. The chemical stability of the calcium phosphate coatings loaded with trehalose was also investigated by incubating the coated samples in phosphate buffered solution (PBS) at 37 °C for short periods ranging from 1 to 30 min. FT-IR spectroscopy and SEM were employed to study possible chemical and morphological changes in the coatings associated with the release of trehalose into PBS.

3. Results and discussion

3.1. Characterizations of as-prepared calcium phosphate coatings

Fig. 1 shows the scanning electron micrographs of the calcium phosphate-coated needles prepared under various calcium and phosphate ion concentrations. It is seen that at all concentrations, the electrochemical process allowed deposition of calcium phosphate over the entire surface of needles in contact with the electrolyte, including the needle tips. As expected, the rate of nucleation and growth of calcium phosphate crystals

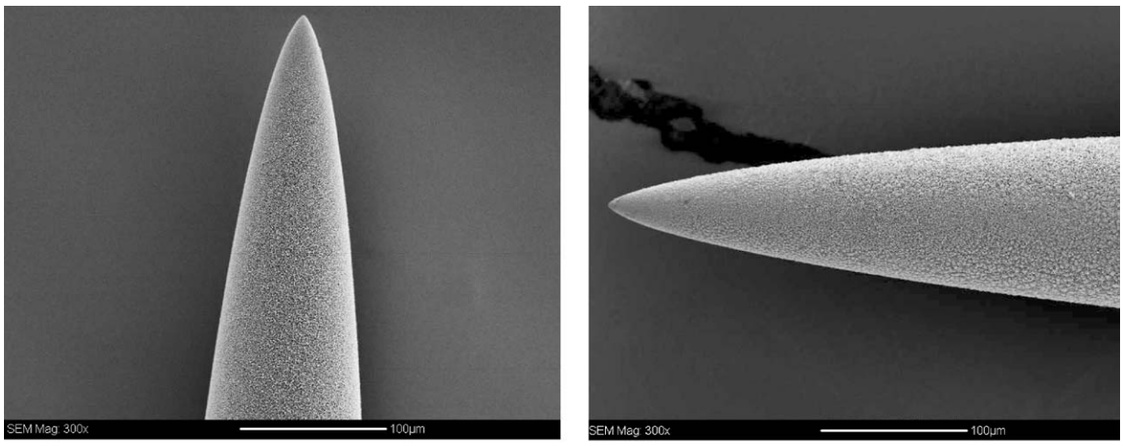

(a) (b)

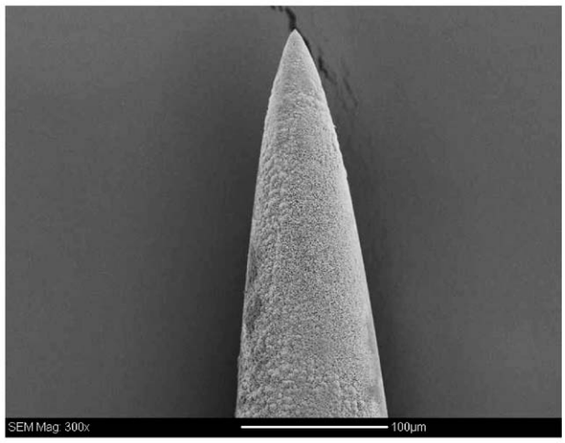

(c)

Figure 1 Scanning electron micrographs of the calcium phosphate-coated needles prepared under varying calcium ion concentrations: (a) API, (b) APII, and (c) APIII.

was relatively faster in more concentrated electrolytes. Thus, at the highest concentrations of calcium and phosphate ions used in this work, a coating time of only 5 min was sufficient to obtain a uniform coating with an average thickness of about 1 um close to the needle tip. In contrast, a much longer coating time ($t > 2$ h) was required to uniformly coat the needles with a comparable thin film of calcium phosphate in more dilute electrolytes.

Fig. 2 shows the surface morphology of the coatings close to the tips of needles at a higher magnification. As seen in this figure, marked changes in the morphology and crystal structure of calcium phosphate coatings were observed as the concentrations of calcium and phosphate ions were lowered. At the highest concentrations of calcium and phosphate ions, coatings formed (API) appeared to be highly porous and consisted of small, loosely packed plate- like crystals of calcium phosphate (Fig. 2(a)). These crystals had a size ranging from 0.2–0.5 um close to the needle tip. The FT-IR spectrum of these coatings (Fig. 3(a)) showed, in addition to the bands associated with hydroxyapatite (HA) (1100–1032, 962, 3570 cm^{-1}) (7), bands attributed to octacalcium phosphate (OCP) (525 and 900–865,and 1280 cm^{-1}) very close to those reported for OCP (8). The appearance of both OCP and HA bands in the FT-IR spectrum of API may signify the presence of OCP-apatite inter-layering similar to biological apatite.

At lower concentrations of calcium and phosphate ions, coatings formed (APII and APIII) appeared to be relatively more compact (Fig. 2(b) and (c)). The FT-IR spectra of these coatings (Fig. 3(b) and (c)) also appeared to be quite different from API. Generally, as the concentration of the electrolyte decreased, the infrared bands at 961, 1050, and 1100 cm^{-1}, corresponding to hydroxyapatite, became more resolved and intense. Also, the intensity of the peak at 925 cm^{-1} corresponding to acid phosphate groups gradually decreased as the concentration was lowered. Based on the FT-IR and SEM results, micro-porous calcium phosphate coatings obtained at low concentrations are expected to be chemically and mechanically more stable than those prepared at higher concentrations.

3.2. Characterization of calcium phosphate coatings loaded with trehalose

Fig. 4 shows the morphology of a typical calcium phosphate coating (API) after treatment in 10%

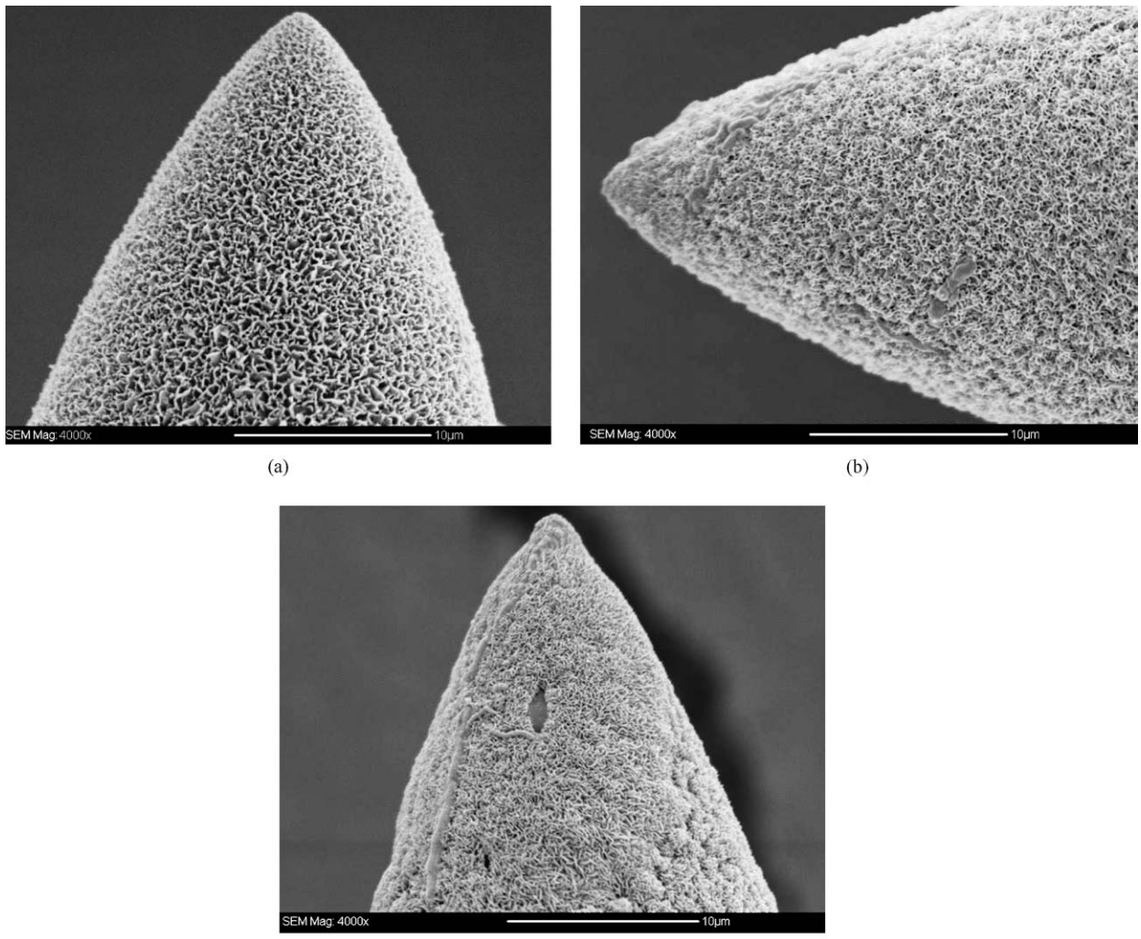

Figure 2 High magnification (×4000) scanning electron micrographs showing the porous structure of the calcium phosphate coatings close to the tip of the needles: (a) API, (b) APII, and (c) APII.

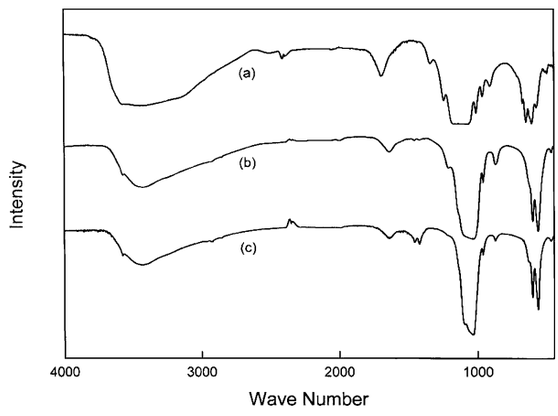

Figure 3 FT-IR spectra of the as-prepared calcium phosphate coatings: (a) API, (b) APII, and (c) APIII.

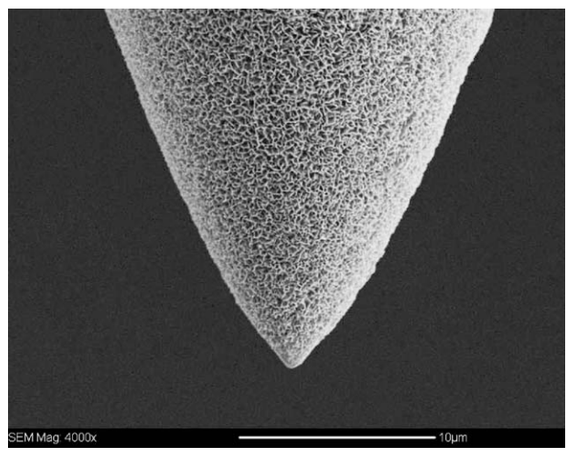

Figure 4 Scanning electron micrograph of a typical API-coated needle after treatment in 10% trehalose solution.

trehalose solution. As seen in this figure, trehalose appears to be incorporated in the calcium phosphate coating in the form of a thin film without significantly affecting the porous structure of the coating. FT-IR spectra of the API treated in trehalose solutions at various concentrations are shown in Fig. 5. For reference, FT-IR spectra of the solid trehalose and the API coating are also presented in the same figure (Fig. 5(a) and (b), respectively). Referring to the IR spectrum of trehalose, the bands at 3500 cm^{-1} and 1680 cm^{-1} are assigned to the stretch vibration and the H─O─H bending of the two crystal water molecules in the trehalose dihydrate

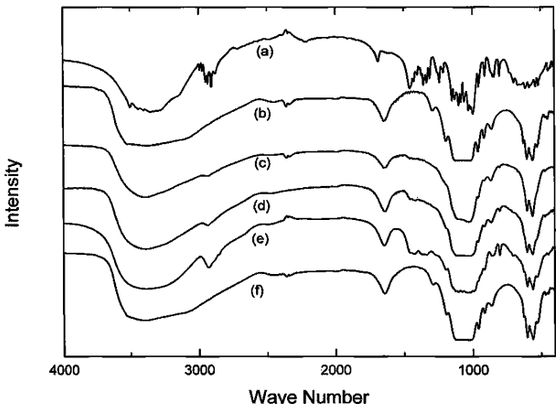

Figure 5 FT-IR spectra of: (a) solid trehalose, (b) API, (c) API treated in 2% trehalose, (d) API treated in 5% trehalose, (e) API treated in 20% trehalose, and (f) API treated in 20% trehalose and incubated in PBS for 1 min.

molecule, respectively [9]. The bridge C─O─C stretching modes of trehalose occur between 1200 and 900 cm^{-1} [10]. As seen in Fig. 5(c)–(e), these bands extensively overlapped with the IR bands associated with the P─O groups of the calcium phosphate. Therefore, in the present work, instead of using the intensity of the bands associated with the bridge C─O─C stretching modes, the intensity of the CH stretching band at 2910–2965 cm^{-1} was used to obtain a measure of amount of trehalose incorporated in the porous calcium phosphate coatings. As seen in Fig. 5(c)–(e), the intensity of the CH stretching band increased with the concentration of the trehalose in the solution, indicating higher loading in more concentrated trehalose solutions. However, at all concentrations, the IR bands corresponding to P─O groups of the calcium phosphate coating did not noticeably shift upon adsorption of trehalose molecules, indicating no chemical interaction between trehalose and the porous calcium phosphate coating. Similar results were also obtained for other calcium phosphate coatings (APII and APIII) prepared at lower concentrations. It appears, therefore, that hydrogen bonding is the most likely driving force for the adsorption of trehalose on porous calcium phosphate coatings. Further support for this view comes from the short-term incubation tests in the PBS solution. As shown in Fig. 5(f), incubation of the calcium phosphate coatings loaded with trehalose in the PBS at 37 °C resulted in the rapid rehydration and complete release of trehalose in a very short time (1 min.). It is noted that the IR spectrum of the calcium phosphate coating after the complete release of trehalose is very similar to the IR spectrum of the untreated calcium phosphate coating (Fig. 5(b)). These results indicate that trehalose may be reversibly adsorbed into the porous calcium phosphate coating without significantly altering the chemical composition of the coating. The FT-IR results further confirmed that the solid trehalose incorporated into porous coatings in the form of a thin film would dissolve rapidly in presence of water, and thus may act as a fast-dissolving reservoir for the extracellular delivery of bioactive agents in the epidermis.

3.3. Skin tests

Fig. 6(a) is the scanning electron micrograph of a typical APII-coated needle treated in 40% trehalose solution that was inserted into skin and removed after 5 s. For comparison, the morphology of the coated needle prior to the skin test is also shown in Fig. 6(b). The coated needle penetrated the skin by locally disrupting the stratum corneum. The local disruption of the stratum corneum was manifested by the release of the intact corneocytes from the stratum corneum. As shown in Fig. 6(a), corneocytes released from the stratum corneum were often seen to be attached to the coated needles. The imposed local high strain to the stratum corneum appears to be responsible for the loss of cohesion and the detachment of corneocytes from the intercellular lipid multilayers. These results indicate that the bonding between corneocytes and the intercellular lipid multi-layers is weaker than the intrinsic resistance of corneocytes themselves. These observations are in line with the 'bricks and mortar' theory, in which corneocytes comprise the 'bricks', embedded in a 'mortar', composed of multilayers of ceramides, fatty acids, cholesterol and cholesterol esters [11, 12].

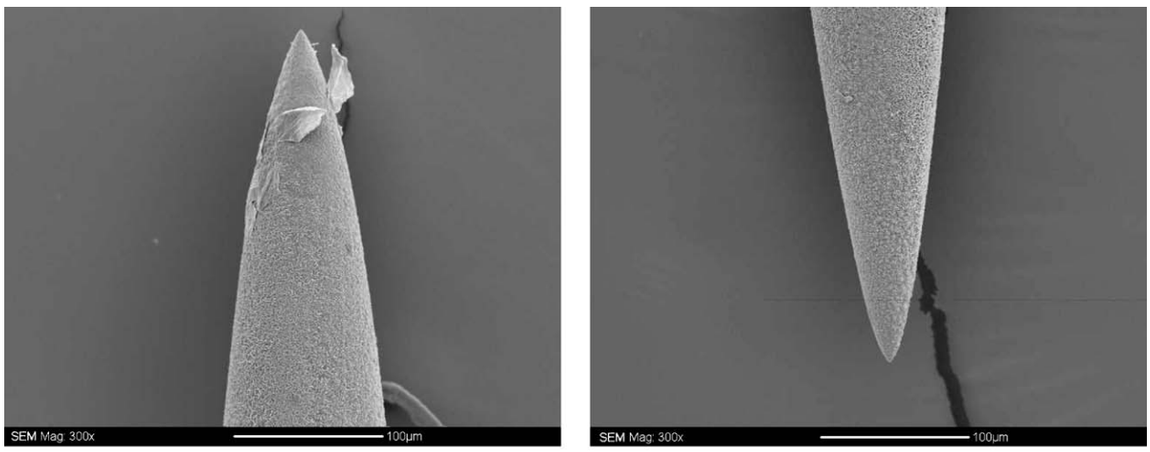

(a) (b)

Figure 6 Scanning electron micrograph of a typical APII-coated needle treated in 40% trehalose: (a) after the skin test, and (b) before the skin test.

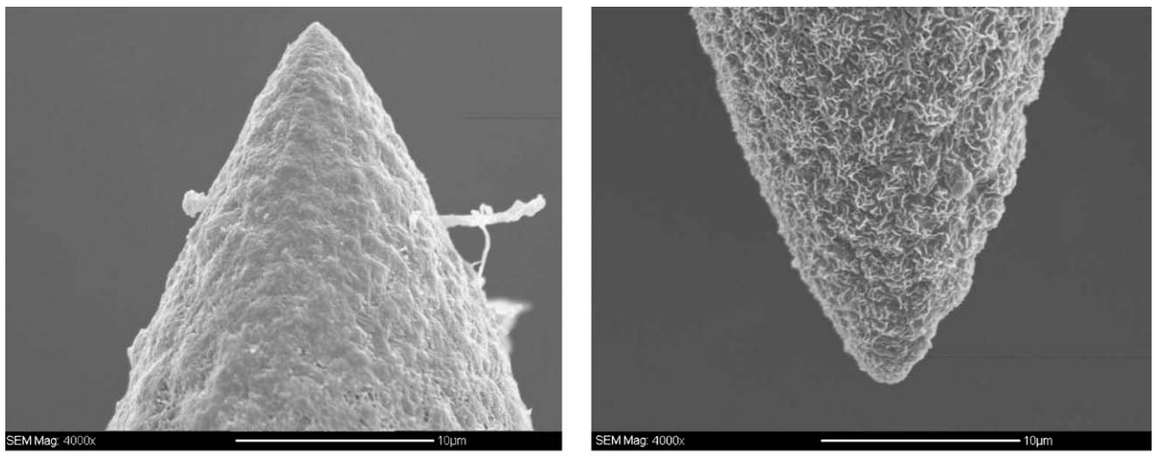

(a) (b)

Figure 7 (a) High magnification SEM micrograph of a typical APII-coated needle treated in 40% trehalose: (a) after the skin test, and (b) before the skin test.

Based on the SEM observation of the corneocytes attached to the coated needle (Fig. 6(a)), the minimum depth of penetration into skin was estimated to be about 120 μm. In humans, the stratum corneum is about 10 to 20 μm in thickness, with the underlying epidermis layer ranging from 50 to 150 μm [4]. Therefore, a depth of penetration of 120 μm should be sufficient for breaching the stratum corneum layer and delivering the solid trehalose to the epidermis without stimulating the nerves in deeper tissues. As seen in Fig. 6(a), the calcium phosphate coating remained largely intact and attached to the needle and there was no sign of cracking or physical fragmentation of the coating as a result of insertion into skin. The surface morphology of the coating, however, was noticeably changed close to the needle's tip (Fig. 7(a)) as a result of the rehydration of trehalose in the epidermis. The porous coating also appears to be compressively deformed in response to the high level of interfacial stress during penetration of the needle into skin. Other factors such as in vivo protein adsorption, dissolution/precipitation of calcium phosphate, and interaction with the rehydrated trehalose in the epidermis may also be partly responsible for the observed morphological changes. However, chemical interactions are not expected to play major roles since the coated needles were embedded in skin only for a very short time (5 s). SEM observations of the coated needles incubated in the PBS at 37 °C confirmed that although trehalose may be completely released in a very short time (1 min), the porous structure of the calcium phosphate coating does not seem to be affected in PBS (Fig. 8). It appears, therefore, that the morphological changes observed in Fig. 6(a) are mainly associated with the rehydration of trehalose and compressive deformation of the coating.

Fig. 9 shows the SEM micrograph of the APII- coated needle treated in 40% trehalose solution which was inserted into the skin to a depth greater than 300 μm and left embedded in skin for a relatively longer time (30 s). It is seen that even under these severe conditions the coating remained largely intact and attached to the needle. The coating morphology was altered but the coating did not break during the penetration into skin. As noted previously, trehalose is capable of forming strong hydrogen bonds with the porous calcium phosphate coatings and is, therefore, expected to

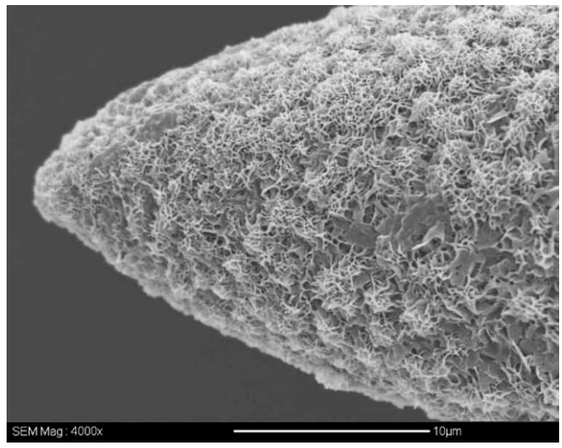

Figure 8 Scanning electron micrograph of a typical APII-coated needle after incubation in PBS for 1 min (coating was treated in 40% trehalose solution).

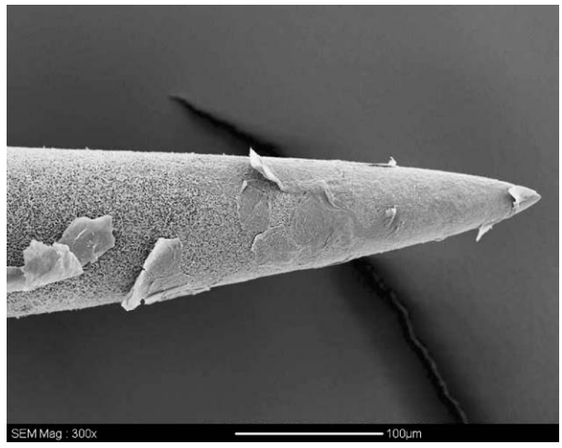

Figure 9 Scanning electron micrograph of a typical APII-coated needle after the skin test (coating was treated in 40% trehalose solution).

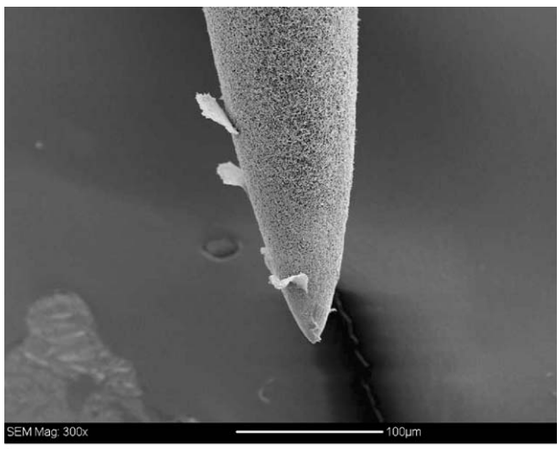

(a)

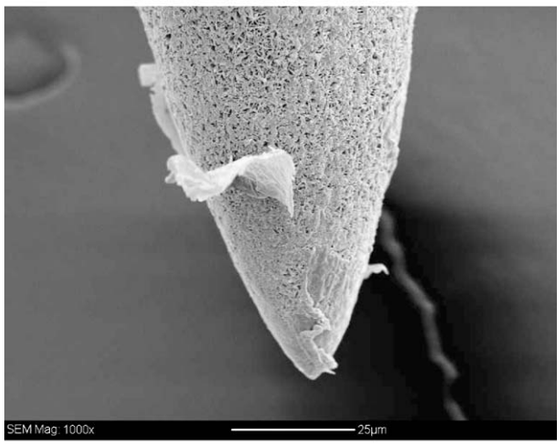

(b)

Figure 10 Scanning electron micrograph of a typical APII-coated needle without trehalose after the skin test: (a) ×300, and (b) ×1000.

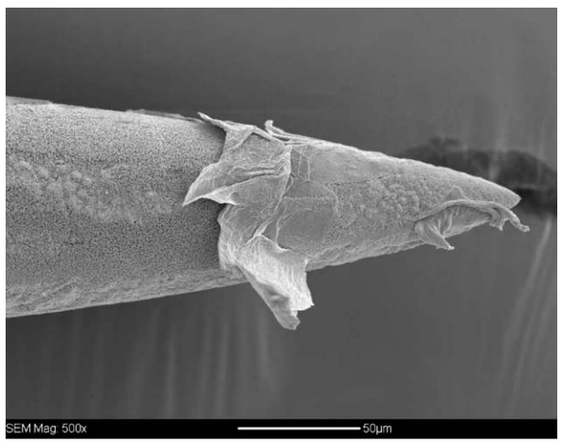

(a)

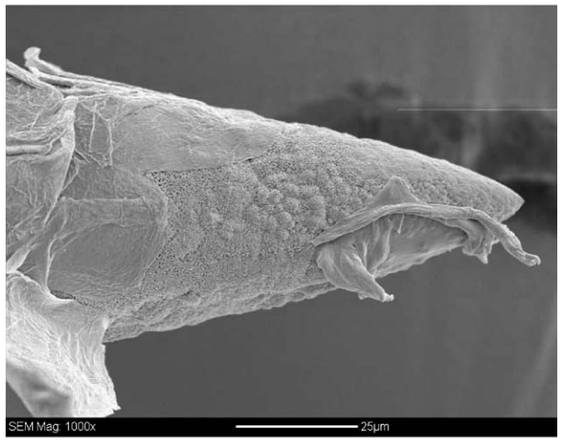

(b)

Figure 11 Scanning electron micrograph of a typical APIII-coated needle without trehalose after the skin test: (a) ×500, and (b) ×1000.

significantly improve the cohesive strength of these coatings under dry conditions. However, once transported below the stratum corneum, trehalose would rapidly dissolve within the epidermis where the water content can reach as high as 70% [13]. Thus, although trehalose may act as an effective binder during the initial penetration of the needle into the stratum corneum, it does not significantly contribute to the mechanical stability of the porous calcium phosphate coating within the epidermis. To validate this view, coated needles without trehalose were also inserted into skin under similar conditions. Fig. 10 is the scanning electron micrograph of a typical APII-coated needle without trehalose that was inserted into skin to a depth of about 200 μm and removed after 5 s. It can be seen that even in the absence of trehalose, the porous calcium phosphate coating remained largely intact and attached to the needle. These findings indicate that by controlling the processing parameters, it should be possible to synthesise porous calcium phosphate coatings with sufficient mechanical strength that would cross the stratum corneum barrier without the need for a binding agent. Indeed, by simply reducing the calcium and phosphate ion concentrations in the electrolyte, coatings with lower porosity and improved cohesion strength were synthesized. Fig. 11 is the scanning electron micrograph of a typical APIII-coated needle prepared at [Ca] = 0.5 mM which was inserted into skin to a depth of about 100 μm and removed after 5 s. It is seen that the trehalose-free coating prepared under these conditions penetrated the stratum corneum with minimum surface morphological changes.

In contrast to the above results, API-coated needles prepared at the highest concentrations of calcium and phosphate ions suffered extensive mechanical damage during penetration into skin presumably due to the weak cohesion strength of the coating (Fig. 12). Extensive mechanical damage also occrred when API-coated needles pierced through a 300 μm thick latex film under dry conditions (Fig. 13(a)). As shown in Fig. 13(b), post-treatment of the coated needle in the trehalose solution significantly improved the mechanical performance of the coating under dry conditions. This treatment, however, did not improve the mechanical performance of the coating within the epidermis. Fig. 14 is the micrograph of a typical API-coated needle loaded with dried trehalose that was inserted into skin to a depth of about 300 μm and removed after 5 s. It is seen that in this case, upon removal of the needle from skin, the calcium phosphate coating was completely

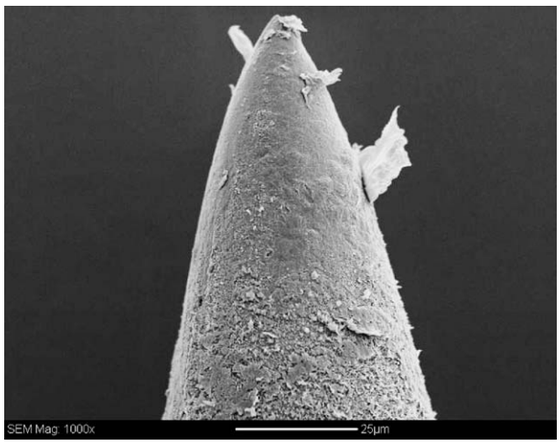

Figure 12 Scanning electron micrograph of a typical API-coated needle without trehalose after the skin test.

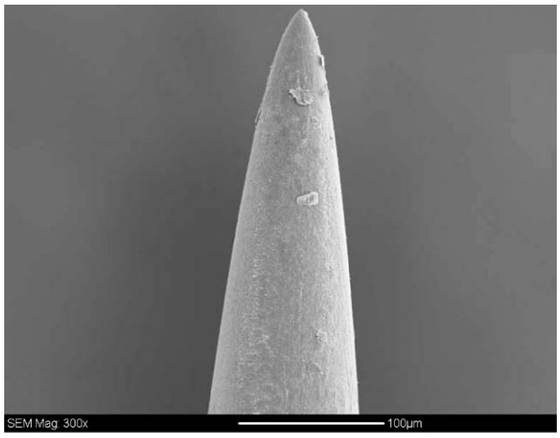

(a)

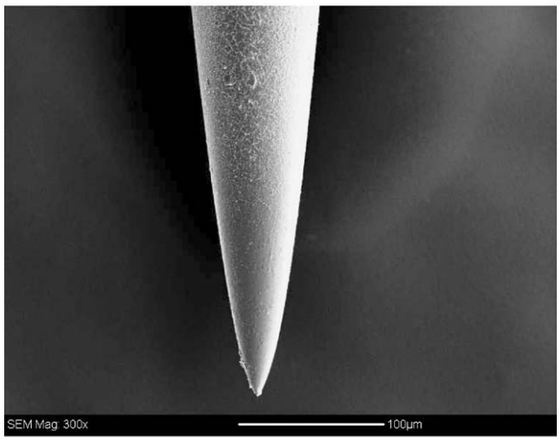

(b)

Figure 13 Sanning electron micrograph of a typical API-coated needle after piercing through latex film: (a) API without trehalose, and (b) API with trehalose.

released from the needle and left behind in the skin. The exact mechanism of the release of the API coating in the epidermis is not well understood at this time but it may be associated with the rapid rehydration of the trehalose below the stratum corneum and weakening of the bond at coating-substrate interface. Rehydrated trehalose may further bridge the calcium phosphate

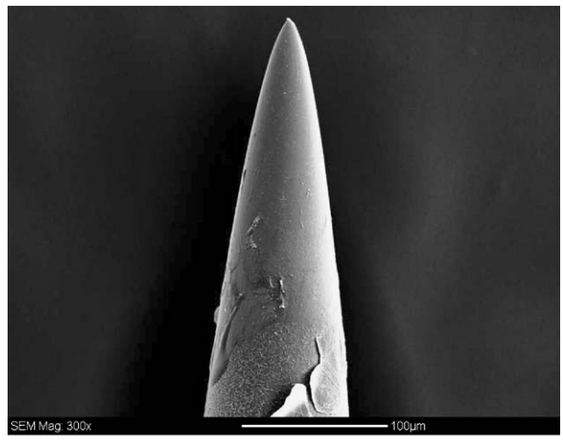

(a)

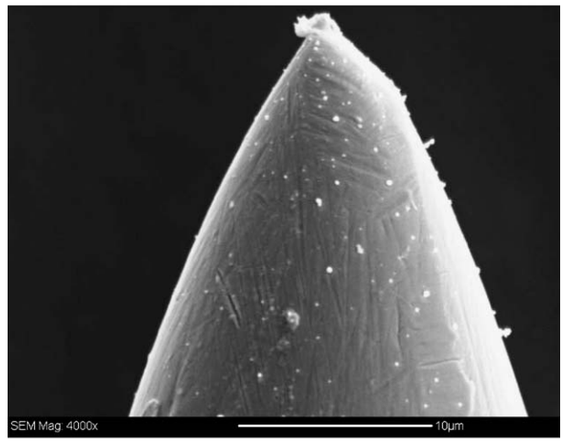

(b)

Figure 14 Scanning electron micrograph of a typical API-coated needle after the skin test (coating was treated in 10% trehalose solution): (a) $\times$300, and (b) $\times$4000.

coating to the adjacent intercellular components of the epidermis through the formation of hydrogen bonds. These bonds appear to be much stronger than the interfacial bonds that exist at the coating-substrate interface.

It should be emphasised that the complete detachment and release of the coating in the epidermis was only observed in the case of API coatings that contained solid trehalose. These findings demonstrate that by optimizing the processing parameters, trehalose-containing calcium phosphate coatings with appropriate degrees of porosity and cohesion strength may be synthesized that can be controllably released within the epidermis in a relatively short time. In the present work, it is not clear whether the calcium phosphate coating is released in one piece or if it is disintegrated into smaller fragments upon removal of the needle from the skin. Whatever mechanism is involved, it is expected that in the long term the fine calcium phosphate crystals left embedded in the epidermis will eventually be taken up by the epidermal cells, including epidermal Langerhans cells (LHC).

The possibility of controllably releasing fine calcium phosphate particles within the epidermis using calcium phosphate-coated microneedles opens up an alternative

route for delivering protein antigen and nucleic acid molecules to the epidermis. Thus while solid trehalose incorporated into the porous calcium phosphate coatings may be used as a fast-dissolving reservoir for extracellular delivery of bioactive agents, calcium phosphate crystals may also be adapted as solid microcarriers for particle-mediated, intracellular delivery of the bioactive materials into the epidermis. Indeed, the physicochemical properties of porous calcium phosphate coatings would allow direct immobilization of a wide range of bioactive molecules on calcium phosphate crystals, including DNA molecules. It is known that calcium phosphate can form ionic complexes with the nucleic acid backbone and that the DNA/calcium phosphate complexes may be carried across cell membrane via ion channel mediated endocytosis [14]. Calcium phosphate- coated microneedles loaded with trehalose may therefore provide a simple mechanism for the intracellular delivery of DNA molecules into the epidermis in comparison with the delivery systems that employ driving forces such as ballistic energy [15].

4. Conclusions

The results in this work provide the first in vivo use of microporous calcium phosphate coatings to deliver solid trehalose to the epidermis. Microporous calcium phosphate coatings deposited on needles and loaded with trehalose effectively breached the stratum corneum and allowed direct access to the epidermis without breaking during insertion into skin. The visual examination of the skin at the site of the needle entry showed no sign of skin reactions, bleeding or infection over the days that followed. Thus the insertion of the coated needle into the skin would appear to be minimally invasive and well tolerated. Due to their biocompatibility and high capacity for absorption of water, these coatings may be useful for immobilizing vaccine ingredients including solid antigen reservoirs on arrays of micro-needles using newly emerging technologies such as inkjet printing.

Acknowledgment

The author thanks Natural Science and Engineering Research Council of Canada (NSERC) for the financial support provided for this research project. The author also wishes to thank Jenny Yin for her assistance in preparation of samples for the FT-IR and SEM analysis.

References

1. S. BABUIK, M. BACA-ESTRADA, L. A. BABUIK, C. EWEN and M. FOLDAVI, *J. Control. Release* **66** (2000) 199.
2. S. HENRY, D. V. MCALLISTER, M. G. ALLEN and M. R. PRAUSNITZ, *J. Pharm. Sci.* **87** (1998) 922.
3. J. A. MARTRIANO, M. CORMIER, J. JOHNSON, W. A. YOUNG, M. BUTTERY, K. NYAM and P. E. DADDONA, *Pharm. Res.* **19** (2002) 63.
4. M. SHIRKHANZADE and M. AZADEGAN, *J. Mater. Sci: Mater. in Med.* **9** (1998) 385.
5. M. SHIRKHANZADEH, *ibid.* **9** (1998) 67.
6. Y.-H. LIAO, M. B. BROWN, T. NAZIR, A. QUADER and G. P. MARTIN, *Pharm. Res.* **19** (2002) 1847.
7. J. ARENDS, J. CHRISTOFFERSEN, M. R. CHRISTOFFERSEN, H. ECKERT, B. O. FOWLER, J. C. HEUGHEBAERT, G. H. NANCOLLAS, J. P. YESINOWAKI and S. ZOWAKI, *J. Crystal. Growth* **84** (1987) 515.
8. B. O. FOWLER, E. C. MORENO and E. BROWN, *Arch. Oral. Biol.* **11** (1966) 477.
9. K. AKAO, Y. OKUBO, T. IKEDA, Y. INOUE and M. SAURAI, *Chem. Lett.* **8** (1998) 759.
10. M. SEKKAL, V. DINCQ, P. LEGRAND and J. P. HUVENNE, *J. Mol. Struct.* **349** (1995) 349.
11. P. M. ELIAS, *J. Invest. Dermatol.* **80** (1983) 445.
12. V. A. ZIBOH, *Lipids* **31** (Suppl.) (1996) S249.
13. P. J. CASPERS, G. W. LUCASSEN, H. A. BRUINING and G. J. PUPPELS, *J. Raman Spectrosc.* **31** (2000) 818.
14. V. L. TRUONG, S. M. WALSH, E. SCHWABERT, H. Q. MAO, W. B. GUGGINO, J. T. AUGUST and K. W. LEONG, *Biochem. Biophys.* **361** (1999) 47.
15. S. KURIYAMA, A. MITORO, H. TSUJINOUE, T. NAKATANI, H. YOSHIJI, T. TSUJIMOTO, M. YAMAZAKI and H. FUKUI, *Gene Therapy* **7** (2000) 1132.

Received 5 January
and accepted 20 May 2004